J. Biochem. **139**, 597–605 (2006)
doi:10.1093/jb/mvj063

Saccharomyces cerevisiae Rot1p Is an ER-Localized Membrane Protein That May Function with BiP/Kar2p in Protein Folding

Masato Takeuchi[1], Yukio Kimata[1], Aiko Hirata[2], Masahiro Oka[1,*] and Kenji Kohno[1,†]
[1]Graduate School of Biological Sciences, Nara Institute of Science and Technology (NAIST), 8916-5 Takayama, Ikoma, Nara 630-0192; and [2]Department of Integrated Biosciences, Graduate School of Frontier Sciences, University of Tokyo, 5-1-5, Kashiwanoha, Kashiwa, Chiba 277-8562

Received January 6, 2006; accepted January 28, 2006

The 70-kDa heat shock protein (Hsp70) family of molecular chaperones cooperates with cofactors to promote protein folding, assembly of protein complexes and translocation of proteins across membranes. Although many cofactors of cytosolic Hsp70s have been identified, knowledge about cofactors of BiP/Kar2p, an endoplasmic reticulum (ER)–resident Hsp70, is still poor. Here we propose the *Saccharomyces cerevisiae* protein Rot1p as a possible cofactor of BiP/Kar2p involved in protein folding. Rot1p was found to be an essential, ER-localized membrane protein facing the lumen. *ROT1* genetically interacted with several ER chaperone genes including *KAR2*, and the *rot1-2* mutation triggered the unfolded protein response. Rot1p associated with Kar2p, especially under conditions of ER stress, and maturation of a model protein, a reduced form of carboxypeptidaseY, was impaired in a *kar2-1 rot1-2* double mutant. These findings suggest that Rot1p participates in protein folding with Kar2p. Morphological analysis of *rot1-2* cells revealed cell wall defects and accumulation of autophagic bodies in the vacuole. This implies that the protein folding machinery in which Rot1p is involved chaperones proteins acting in various physiological processes including cell wall synthesis and lysis of autophagic bodies.

Key words: co-chaperone, endoplasmic reticulum, Hsp70, molecular chaperone, protein folding, unfolded protein response.

Abbreviations: CPY, carboxypeptidase Y; EndoH, endoglycosidase H; ER, endoplasmic reticulum; ERAD, ER-associated degradation; 5-FOA, 5-fluoroorotic acid; Hsp, heat shock protein; sRot1p, smaller form of Rot1p; Tm, tunicamycin; UPR, unfolded protein response.

Among molecular chaperones, the 70-kDa heat shock protein (Hsp70) family is known to play a central role in folding of nascent proteins. Hsp70s are composed of two main regions: an ATPase domain on the N-terminal side and a peptide-binding domain on the C-terminal side. It is widely believed that Hsp70s repeatedly bind and release unfolded protein substrates in a cycle coupled to, and dependent on, their ATPase cycle (*1*). Hsp70s cooperate with various cofactors. Most of them are reported to modulate the ATPase cycle of the Hsp70s, thereby regulating binding and release of substrate proteins. J proteins (Hsp40s) are the most prominent partners of Hsp70s (*2*), and the nucleotide exchange factors (NEFs) are also important cofactors (*3*). Furthermore, Hsp70 cofactors designated Hip, Hop and CHIP have been identified in the mammalian cytosol (*4–6*). The existence of such a variety of cofactors suggests that Hsp70s in the eukaryotic cytosol are regulated in a complex fashion.

BiP is an endoplasmic reticulum (ER)-resident Hsp70 family protein that is evolutionally conserved among eukaryotes. In the budding yeast *Saccharomyces cerevisiae*, BiP is encoded by *KAR2*; and BiP/Kar2p is known to be involved in multiple steps of maturation of newly-synthesized proteins in the ER. First, BiP/Kar2p functions in translocation of nascent proteins into the ER, where it is recruited to the translocon by the J protein Sec63p (*7*). Second, BiP/Kar2p facilitates protein folding in the ER (*8*). Third, BiP/Kar2p contributes to the quality control system that retains abnormal proteins in the ER and/or sends them back to the cytosol for degradation by the proteasome [so-called ER-associated degradation (ERAD)] (*9*, *10*). Two other ER-localized J proteins, Scj1p and Jem1p, are reported to function with BiP/Kar2p in protein folding and ERAD (*11*, *12*). In addition to J proteins, two NEFs for Kar2p, Lhs1p and scSls1p/Sil1p, have been identified in yeast (*13*, *14*). Kar2p requires at least one NEF to facilitate nascent protein translocation (*15*). Lhs1p is a distant relative of Hsp70s (*16*), and may also participate in protein folding in the ER (*17*). Kar2p cofactors other than J proteins and NEFs have not yet been identified.

Here we describe a search for novel Kar2p cofactors and characterization of a candidate protein, Rot1p.

MATERIALS AND METHODS

Strain Construction—Plasmids used in this study were generally constructed by subcloning genomic PCR products into yeast vectors, and are listed in Table 1. Yeast strains were grown in complete (YPD), synthetic (SD) or synthetic

*Present address: Department of pathology, University of Florida College of Medicine, Gainesville, FL 32610-0275, USA.
†To whom correspondence should be addressed. Tel: +81-743-72-5640, Fax: +81-743-72-5649, E-mail: kkouno@bs.naist.jp

Table 1. **Plasmids.**

Name	Backbone (cloning sites)	Cloned fragment(s)
pK2D2	pRS305[a]	*KAR2* (−1934∼+33[b]; *Sac*I/*Xba*I)
	(*Sac*I/*Xba*I/*Hin*dIII)	(+2079∼3161; *Xba*I/*Hin*dIII)
pCUA3K2	pCH1122[c] (*Sal*I)	*KAR2* (−1282∼+3935)
pRS314-*KAR2*[c]	pRS314[a] (*Sac*I/*Xho*I)	*KAR2* (−1282∼+3935; *Sac*I/*Sal*I)
pCL2	pBluescript II SK(−)[e]	*CEN*/*ARS* cassette[f] and
	(*Nae*I)	*LYS2* (−295∼+4335)
pCL2-*kar2-1*	pCL2 (*Sac*I/*Sal*I)	*kar2–1*(−1282∼+3935)
pRS314-*ROT1*	pRS314 (*Eco*RV)	*ROT1* (−508∼+1022)
pRS316-*ROT1*	pRS316 (*Sac*I /*Sal*I)	*ROT1* (−508∼+1022)
pCL2-*ROT1*	pCL2 (*Spe*I/*Cla*I)	*ROT1* (−484∼+1117)
pCL2-*rot1–2*	pCL2 (*Spe*I/*Cla*I)	*rot1–2* (−484∼+1117)
pT-*ROT1-HA*	pGCT10[g] (*Spe*I/*Pst*I)	*ROT1* (−484∼+768)-*3HA-stop*
pT-*rot1–2-HA*	pGCT10 *(Spe*I/*Pst*I)	*rot1–2* (−484∼+768)-*3HA-stop*
pRD2	pRS305	*ROT1* (−1764∼−114; *Spe*I/*Hin*dIII)
	(*Hin*dIII/*Spe*I/*Sac*II)	(+1023∼+2266; *Eco*RV/*Spe*I)
pKCH	pRS303[a]	*CNE1* (−1838∼−;23; *Xho*I/*Bam*HI)
	(*Xho*I/*Bam*HI/*Not*I)	(+1546∼+2903; *Bam*HI/*Not*I)
pKSJH	pRS303	*SCJ1* (−1200∼−1; *Xho*I/*Bam*HI)
	(*Xho*I/*Bam*HI/*Not*I)	(+2270∼+3300; *Bam*HI/*Not*I)
pLD2	pRS305	*LHS1* (−1093∼−580; *Hin*dIII/*Apa*I)
	(*Apa*I/*Hin*dIII/*Sma*I)	(+1630∼+2500; *Hpa*I/*Hin*dIII)
pRS426-*CNE1*	pRS426[a] (*Not*I)	*CNE1* (−330∼+1830)
pRS426-*SCJ1*	pRS426 (*Not*I)	*SCJ1* (−260∼+1570)
pL-*GFP-ATG8*	pANL10[b] (*Bam*HI/*Eco*RI)	*ATG8* (+1∼+354)
pQE-*ROT1*	pQE80L[h] (*Bam*HI/*Sal*I)	*ROT1* (+73∼+693)

[a]Sikorski and Hieter, 1989. [b]ORF starts at +1. [c]Wimmer *et al*., 1992. [d]*KAR2* in pRS314-*KAR2* was excised by *Xho* I and replaced by *kar2-1* to generate pRS314-*kar2-1*. [e]Stratagene. [f]Amplified by PCR from pRS314. [g]Iha and Tsurugi, 1998. [h]Qiagen.

Table 2. **Yeast strains.**

Strain	Genotype
CH1462[a]	*Matα ade2 ade3 his3 leu2 ura3*
FY23[b]	*Mat***a** *leu2 trp1 ura3*
YM5	*Mat***a** *ade2 ade3 his3 leu2 lys2 trp1 ura3 kar2*Δ*::LEU2* (pCUA3K2)
YM6	*Mat***a** *ade2 ade3 his3 leu2 lys2 trp1 ura3 kar2*Δ*::LEU2* (pCUA3K2)
YM7	*Mat***a** *ade2 ade3 his3 leu2 lys2 trp1 ura3 kar2*Δ*::HIS3* (pCUA3K2[c], pCL2-*kar2-1*[d])
YM8	*Mata ade2 ade3 his3 leu2 lys2 trp1 ura3 kar2*Δ*::HIS3* (pCUA3K2, pCL2-*kar2-1*)
YMS58	*Mata ade2 ade3 his3 leu2 lys2 trp1 ura3 kar2*Δ*::HIS3 rot1-2* (pCUA3K2, pCL2-*kar2-1*)
YM11	*Mata ade2 ade3 his3 leu2 lys2 trp1 ura3 kar2*Δ*::HIS3 rot1*Δ*::LEU2* (pCUA3K2, pRS314-*ROT1*[e])
YM12	*Mata ade2 ade3 his3 leu2 lys2 trp1 ura3 rot1*Δ*::LEU2* (pRS316-*ROT1*[f])
YM13	*Mata ade2 ade3 his3 leu2 lys2 trp1 ura3 rot1*Δ*::LEU2* (pT-*ROT1-HA*[g])
YM14	*Mata ade2 ade3 his3 leu2 lys2 trp1 ura3 rot1*Δ*::LEU2* (pT-*rot1-2-HA*)
YM16	*Mata ade2 his3 leu2 lys2 trp1 ura3*
YM18	*Mata ade2 his3 leu2 lys2 trp1 ura3 rot1-2*
YM19	*Mata ade2 ade3 his3 leu2 lys2 trp1 ura3 rot1*Δ*::LEU2* (pCL2-*ROT1*)
YM20	*Mata ade2 ade3 his3 leu2 lys2 trp1 ura3 rot1*Δ*::LEU2* (pCL2-*rot1-2*)

[a]From E. Hurt. [b]From F. Winston. [c]pCUA3K2 (*CEN*/*ARS ADE3 URA3 KAR2*). [d]pCL2-*kar2-1* (*CEN*/*ARS LYS2 kar2-1*). [e]pRS314-*ROT1* (*CEN*/*ARS TRP1 ROT1*). [f]pRS316-*ROT1* (*CEN*/*ARS URA3 ROT1*). [g]pT-*ROT1-HA* (*CEN*/*ARS TRP1 ROT1-HA*).

complete (SC) medium, which was supplemented with 2% agar for growth on plates. Standard genetic manipulations were performed as described (*18*). Yeast strains used in this study are listed in Table 2. CH1462 is an *ade2 ade3* strain used for the colony-sectoring assay, kindly provided by Dr. E. Hurt (Biochemie-Zentrum der Universitat Heidelberg). *kar2* temperature-sensitive mutants (*kar2-113, kar2-133*, *kar2-159*, *kar2-191*) were a generous gift of Dr. M. Rose (Princeton University). CH1462 was crossed with the FY-series strains (from F. Winston, Harvard Medical School) four times to obtain YM-series strains. Strains were constructed by introduction and/or segregation of plasmids, gene disruption, *HO* conversion, crossing with congenic strains, or chemical mutagenesis. Gene disruptions were performed by transformation of the parental strains with the plasmids listed in Table 1, and confirmed by Southern blotting (*KAR2* and *ROT1*) or genomic PCR (*CNE1*, *SCJ1* and *LHS1*). YMS58 is the original *rot1-2* mutant obtained by chemical mutagenesis described below. To obtain YM16 and YM18, YMS58 was crossed with FY23 four times.

Mutagenesis and Screening for kar2-1 Synthetic Lethal Mutants—YM7 and YM8 were mutagenized with ethylmethane sulfonate at a killing rate of about 40%. Cells were spread on SC plates containing 2 μg/ml adenine sulfate, and incubated at 30°C. Screening was performed as described (*19*). Briefly, among 200,000 clones screened, 3,578 non-sectoring colonies were isolated and rechecked for the non-sectoring phenotype on SC plates. The resultant 1,672 clones were incubated in liquid YPD and spotted on SD containing 1 mg/ml 5-fluoroorotic acid (5-FOA). Of these, 118 clones were found to be unable to grow on SD + 5-FOA. These clones were transformed with pRS314-*KAR2* or pRS314-*kar2-1*, and growth on SD containing 5-FOA was determined. Eight clones were found to be viable when transformed with pRS314-*KAR2*, but not with pRS314-*kar2-1* on 5-FOA plates, and these were designated *kar2-1* synthetic lethal mutants. Growth of the mutants on the SD + 5-FOA plates was found to be ambiguous, and the *kar2-1 rot1-2* mutant was found to be viable at 30°C but non-viable at 32°C on YPD plates. The mutants were crossed with YM5 or YM6, analyzed by tetrad dissection, and confirmed to carry a single, recessive mutation. A pRS314-based yeast genomic library (ATCC no. 77164) was introduced into the mutants by

transformation to screen for plasmids that rescue the non-sectoring phenotype.

Production of Anti-Rot1p Antibody—His_6-Rot1p(25-231) was expressed in *Escherichia coli* BL21(DE3) from pQE-*ROT1*. Inclusion bodies were isolated and dissolved in U buffer (50 mM Na_2HPO_4/NaH_2PO_4 pH 8.0, 500 mM NaCl, 6 M urea). His_6-Rot1p was purified successively by Ni-NTA (Qiagen) and Prepforesis (a protein purification system based on disk gel PAGE; ATTO) according to the manufacturers' instructions and dialyzed against US-PBS (phosphate buffered saline containing 4 M urea and 0.1% SDS) and injected into guinea pigs. The antiserum was used in our experiments as anti-Rot1p antibody. Anti-Sec61p was kindly provided by Dr. R. Schekman (University of California, Berkeley). Anti-HA and anti-Kar2p were described previously (*20*, *21*).

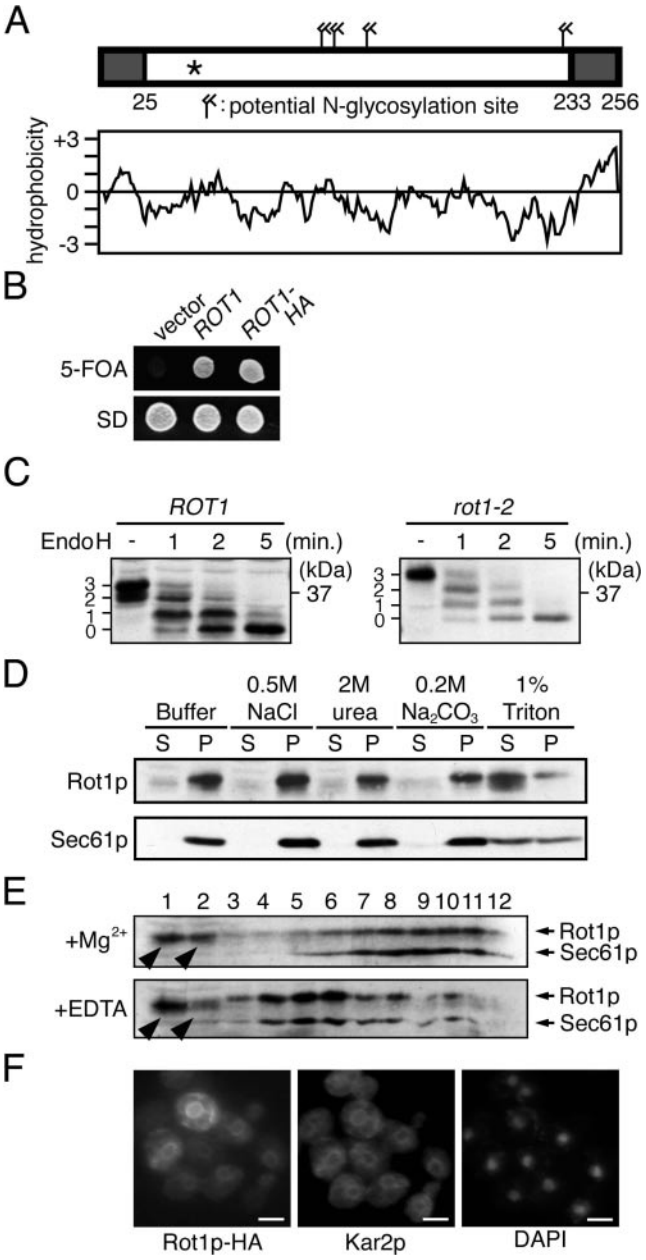

Subcellular Fractionations—Subcellular fractionations were performed as described (*22*, *23*) with a few modifications. Cells were incubated in YPD at 30°C to OD_{600} = 1.5, treated with 10 mM NaN_3 and lysed in LM buffer (10 mM Tris pH 8.0 at 4°C, 150 mM NaCl, 2 mM Mg^{2+}, 10% sucrose) or LE buffer (LM buffer containing 10 mM EDTA instead of Mg^{2+}) at 200 OD_{600} cells/ml by agitation with glass beads. The lysate was centrifuged at 600× *g* for 10 min, and 120 μl of cleared lysate was layered on the top of a 12 ml, 20–60% linear sucrose gradient made in LM or LE buffer. The gradient was centrifuged for 8 h at 150,000× *g* in an SW40Ti rotor (Beckman) and 1 ml fractions were collected manually from the top of the gradient.

Electron Microscopy and Immunofluorescence—Electron microscopic and immunofluorescent analyses were performed as described (*20*). In Fig. 1C, an Axiophoto microscope (Carl Zeiss) equipped with a Plan-Neofluar objective lens (100x/1.3, oil; Carl Zeiss) and a DP70 CCD camera (Olympus) was used. In Fig. 4, E–M, an Apotome system consisting of an Axiovert 200 microscope, a Plan-Apochromat objective lens (100x/1.4, oil), an AxioCam MRm CCD camera and Axio Vision 4 software (Carl Zeiss), was used in the Apotome mode.

Pulse-Chase Experiments—Cells were grown exponentially in SC lacking Met/Cys, concentrated to 5 OD_{600}/ml and further incubated at 37°C for 30 min. The cells were then treated with 5 mM DTT for 15 min and labeled with [^{35}S]-Met/Cys (EXPRESS protein labelling mix; Perkin Elmer) at 2–4 MBq/ml for 10 min at 37°C. At the beginning of the chase period, cells were collected and suspended in SC medium containing 0.4% Met and 0.3% Cys to OD_{600} = 2.0, and incubated at 37°C. Aliquots were taken at the indicated times, and NaN_3 was immediately added to a final concentration of 10 mM. Cells were lysed by

Fig. 1. **Rot1p is an essential ER-localized membrane protein.** (A) Schematic representation and hydrophobicity plot of Rot1p. The N-terminal signal sequence and C-terminal transmembrane region are shown in grey boxes. An asterisk indicates the position of the *rot1-2* mutation (resulting in a single amino acid substitution, G45E). (B) *ROT1* is an essential gene. Δ*rot1* cells (*ura3 trp1*) carrying pRS316-*ROT1* (*CEN*/*ARS*, *URA3*, *ROT1*; YM12) were transformed with the empty vector pRS314 (*CEN*/*ARS*, *TRP1*), pRS314-*ROT1* or pT-*ROT1-HA* (*CEN*/*ARS*, *TRP1*, *ROT1-HA*). The resulting transformants were grown in liquid YPD at 30°C, and aliquots were spotted on SD plates with or without 5-FOA (1 mg/ml; for counter selection of *URA3*). Plates were incubated at 30°C for 1 d and photographed. (C) Rot1p is *N*-glycosylated. The SDS-solubilized lysate of YM16 (*ROT1*) or YM18 (*rot1-2*) was treated with EndoH (20 U/μl) at 37°C for the indicated periods (shown above each panel), and analysed by SDS-PAGE and anti-Rot1p Western blotting to detect Rot1p or rot1-2p. Estimated number of *N*-linked oligosaccharides is shown on the left of each panel. (D) Rot1p is an integral membrane protein. YM16 lysate in buffer LE was incubated with 0.5 M NaCl, 2 M urea, 0.2 M Na_2CO_3 or 1% Triton X-100 at 4°C for 1 h, and fractionated by centrifugation at 100,000 × *g* for 1 h. Rot1p in each fraction was detected as in (C). S, supernatant; P, pellet. (E) Rot1p is localized in the ER. YM16 lysate in LM (+Mg^{2+}) or LE (+EDTA) buffer was fractionated by 20–60% sucrose density gradient centrifugation. The fractions were subjected to Western blotting to detect Rot1p, Sec61p. Arrow heads indicate sRot1p. (F) Indirect immunofluorescence to detect Rot1p-HA and Kar2p. Δ*rot1* cells expressing Rot1p-HA (YM13) were grown in liquid YPD at 30°C, fixed and probed with anti-HA and anti-Kar2p antibodies followed by secondary antibodies conjugated with FITC or rhodamine, respectively. Cells were also stained with DAPI to visualize nuclei. Bars, 5 μm.

agitation with glass beads in 1% SDS-TBES (50 mM Tris, pH 8.0, 5 mM EDTA, 150 mM NaCl), and immunoprecipitation was performed as described (*20*). Labeled proteins were detected with the BAS2500 system (Fujifilm). When DTT was not added, cells were labelled for 5 min and chased similarly. For deglycosylation, immunoprecipitated proteins were eluted with denaturing buffer (0.5% SDS, 1% β-mercaptoethanol) and digested with Endoglycosidase Hf (EndoH; New England Biolabs).

Non-Denaturing Immunoprecipitation—Cells were grown in liquid YPD at 30°C. NaN_3 was added to a final concentration of 10 mM, and the culture was placed on ice for 5 min. Cell harvest, lysis and immunoprecipitation described below were performed at 4°C. Cells were disrupted by agitation with glass beads in 1% Triton X-100-TBES. The lysate was incubated with 1/500 volume of the preimmune serum for 30 min and clarified by centrifugation at 100,000 × *g* for 30 min. It was further incubated with Protein A–Sepharose beads (Amersham Biosciences) for 30 min, and the supernatant was then incubated with 1/500 volume of anti-Kar2p antiserum or preimmune serum. After 1 h of incubation, Protein A–Sepharose beads were added, followed by another 1 h incubation. The beads were then washed five times. Bound proteins were eluted with denaturing buffer, digested with EndoH and detected by Western blotting.

Other Methods—Western blotting, β-galactosidase assay and Northern blotting were performed as described (*21*).

RESULTS

Screening for kar2-1 Synthetic Lethal Mutants—To identify partners of BiP/Kar2p involved in protein folding, we screened for *S. cerevisiae* mutants that exhibited synthetic lethality with the *kar2-1* mutant allele. "Synthetic lethality" refers to a lethal phenotype resulting from the combination of more than one non-lethal mutation. Synthetic lethality of two mutant genes implies that their wild-type versions encode proteins involved in a common cellular function(s). The *kar2-1* mutation corresponds to an amino acid replacement (P515L) in the peptide-binding region of BiP/Kar2p. In *kar2-1* cells, newly synthesized proteins are translocated normally, but the unfolded protein response (UPR) is strongly induced (*21*, *24*). This is likely due to impairment of protein folding in the ER (*25*) and ERAD (*26*). Therefore, screening for mutants synthetically lethal with the *kar2-1* allele was expected to identify factors functionally related to Kar2p, especially those involved in protein folding and/or ERAD.

Following chemical mutagenesis of *kar2-1* cells, screening was performed by the colony-sectoring method (*19*). Among 200,000 clones screened, 8 mutants were obtained that exhibited synthetic lethality (for details, see "MATERIALS AND METHODS"). All the mutants were found to carry recessive, single-gene mutations as confirmed by backcrossing to the parental strain followed by tetrad analysis. Subsequent transformation of the mutants with a wild-type yeast genomic library identified *CDC1*, *KRE6*, *ROT1*, *SEC11* and *SKN1* as the complementing genes. This report focuses on characterization of *ROT1*. While *ROT1* has been shown to be important in 1,6-β-glucan synthesis (*27*, *28*), its specific biochemical function has not been previously determined. Sequencing of the mutant *ROT1* allele identified by the synthetic lethal screen revealed a Gly(45) to Glu replacement (Fig. 1A), which was designated *rot1-2*. Through analysis of a Δ*rot1* mutant carrying plasmid-borne *rot1-2* gene, the *rot1-2* mutation was determined to be responsible for the synthetic lethal phenotype (Fig. 2A).

Rot1p Is an Essential, ER-Localized Membrane Protein—*ROT1* (YMR200w) is essential for vegetative growth under standard culture conditions [Fig. 1B; (*27*)] and encodes a protein of 256 amino acid residues (calculated molecular mass: 28.9 kDa) that is predicted to carry an N-terminal translocation signal sequence, four potential *N*-glycosylation sites and a transmembrane region at the C terminus (Fig. 1A). For characterization of Rot1p, an anti-Rot1p antibody was raised against bacterially expressed His_6-Rot1p(25–231). The lysate of wild-type cells was analysed by Western blotting using the antibody, and Rot1p appeared as two protein bands (Fig. 1C), a major band at 39 kDa and a minor one at

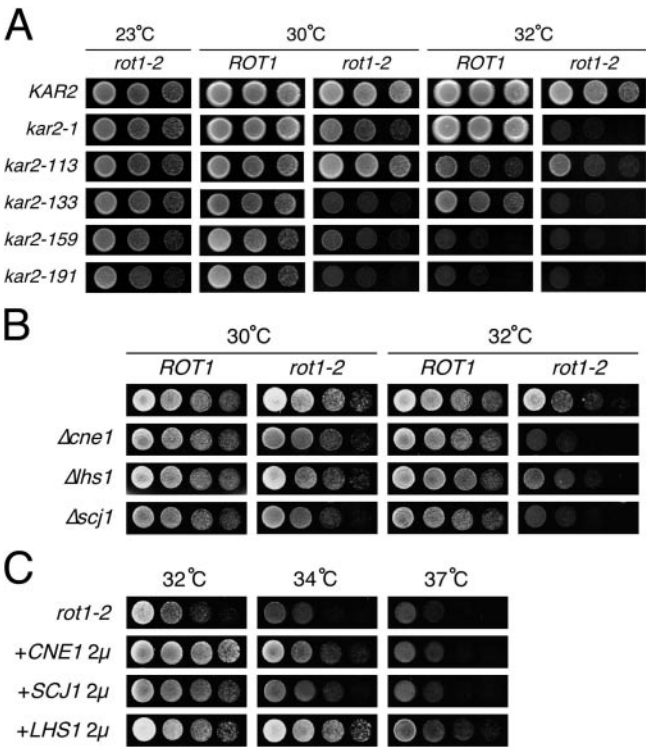

Fig. 2. ***ROT1* genetically interacts with ER-chaperone genes.** (A) Specific alleles of *kar2* are synthetically lethal with *rot1-2*. Δ*kar2* Δ*rot1* cells carrying *KAR2* or one of the *kar2* mutant alleles and *ROT1* or *rot1-2* on centromeric plasmids (pRS314-*KAR2* or *kar2* and pCL2-*ROT1* or *rot1-2*) were generated from YM11 by plasmid shuffling. Cells were grown at 23°C, spotted on YPD plates in a ten-fold dilution series, and incubated at the indicated temperature for 2 d. (B) Synthetic defects of *rot1-2* with Δ*cne1*, Δ*lhs1* or Δ*scj1*. Yeast strains generated from wild-type (YM16) or *rot1-2* (YM18) strains by gene disruption were grown in liquid YPD at 23°C, spotted on YPD plates as a series of five-fold serial dilutions, and incubated at the indicated temperature for 1 d (*ROT1* strains) or 2 d (*rot1-2* strains). (C) Multicopy suppression of *rot1-2* by *CNE1*, *LHS1* and *SCJ1*. Multicopy plasmids (pRS426; 2 μ, *URA3*) carrying *CNE1*, *SCJI or LHS1* were introduced into YM18. The transformants were grown in liquid SC, and temperature sensitivity of growth was assessed as in (B).

37 kDa (referred to as sRot1p for small Rot1p). The number of protein bands of EndoH-digestion intermediates indicates that Rot1p is *N*-glycosylated at three of the four potential sites. The rot1-2p was detected as a single band at 41 kDa and, like Rot1p, found to possess three *N*-linked oligosaccharides (Fig. 1C). The difference in gel mobility between Rot1p and rot1-2p is probably due to the amino acid substitution itself, because bacterially expressed His_6-rot1-2p(25-231) also migrated slower than His_6-Rot1p(25–231) (data not shown). To verify that Rot1p is an integral membrane protein, microsomes were treated with high salt, urea, alkali or detergent, and pelleted (Fig. 1D). Both Rot1p and Sec61p, an ER-localized membrane protein, were extracted only by the detergent treatment, indicating that Rot1p is also an integral membrane protein. The subcellular localization of Rot1p was determined by the sucrose density gradient centrifugation. The detergent-free cell lysate was layered on the top of 20–60% sucrose gradient, centrifuged and fractionated. In the presence of Mg^{2+}, Sec61p was distributed in the heavy fractions, whereas in the presence of EDTA, which causes dissociation of ribosomes from microsomes, Sec61p fractionated in the middle fractions (Fig. 1E). Rot1p co-fractionated with Sec61p in both cases, indicating that Rot1p is localized in the ER. The mutant rot1-2p was also co-fractionated with Sec61p (data not shown). sRot1p, a minor portion of Rot1p, was detected in the lightest fractions, and its localization was unidentified (Fig. 1E). ER localization of Rot1p was also confirmed by indirect immunofluorescent microscopy of the cells expressing Rot1p-HA, in which three repeats of the HA tag was fused to the C terminus of Rot1p. *ROT1-HA* was found to complement the lethal phenotype of the *ROT1* deletion (Fig. 1B), indicating that the tagged protein is functional. Subcellular localization of Rot1p-HA indicated a perinuclear distribution (Fig. 1F), typical of ER-localized yeast proteins. Indeed, Kar2p, an ER resident protein, co-localized precisely with Rot1p-HA (Fig. 1F). Taken together, these results indicate that Rot1p is an essential, predominantly ER-localized, lumen-facing, type-I membrane protein.

Genetic Interaction between Rot1p and ER-Localized Chaperones—The synthetic effects of the *rot1-2* mutation and the previously known *kar2* mutations are shown in Fig. 2A. Because all mutant strains examined here grew at 23°C, cells were initially grown at 23°C, spotted on agar-solidified medium, and further incubated at various temperatures. In combination with *rot1-2*, not only cells harboring *kar2-1*, but those harboring *kar2-133*, *kar2-159* or *kar2-191* were found to grow significantly more slowly at 30°C and 32°C. In contrast, no such synthetic effect was observed in the case of the *kar2-113 rot1-2* double mutant. It should be noted that the phenotypic severity of the individual *kar2* single mutant did not correlate perfectly with the synthetic phenotype in combination with *rot1-2* (compare *kar2-1* and *kar2-133* mutants with *kar2-113* mutants). The allele specificity of synthetic lethality generally implies that two gene products (Kar2p and Rot1p in this case) interact directly to carry out some biological function(s) (*29*).

Potential genetic interactions were then examined between *ROT1* and ER chaperone–encoding genes other than *KAR2*: *CNE1* [encoding a calnexin homologue (30)], *LHS1* and *SCJ1*. As shown in Fig. 2B, Δ*cne1* and Δ*scj1* single mutants exhibited almost normal growth, whereas the double mutants of these genes with *rot1-2* exhibited severe growth defects at 32°C. The combination of Δ*lhs1* and *rot1-2* also resulted in a relatively weak synthetic growth defect. In contrast, disruption of either *JEM1* or *SIL1* did not retard growth of either wild-type or *rot1-2* cells (data not shown).

The *rot1-2* mutation itself caused a growth defect, especially at temperatures above 32°C, which was partly suppressed by multicopy expression of *CNE1*, *LHS1* or *SCJ1* (Fig. 2C). Remarkably, overexpression of *LHS1* enabled the *rot1-2* mutant to proliferate even at 37°C, but did not rescue the lethality of Δ*rot1* (data not shown). Multicopy expression of *JEM1*, *KAR2*, *PDI1*, *SIL1* or *rot1-2* did not cure the growth defect of *rot1-2* cells (data not shown).

ROT1 and ER Stress—Because *ROT1* interacts genetically with several known ER chaperone–encoding genes, it was expected that *rot1-2* cells would exhibit abnormalities related to protein folding in the ER. Accumulation of unfolded proteins in the ER, known as ER stress, triggers transcriptional upregulation of various genes including those encoding ER-resident chaperones and folding enzymes. This defensive mechanism is termed the unfolded protein response (UPR). Induction of the UPR in *rot1-2* cells was monitored using a β-galactosidase reporter (*21*) in which expression of *lacZ* is controlled by a promoter element (termed the UPR element) commonly carried by UPR target genes (*24*). As shown in Fig. 3A, *rot1-2* cells exhibited higher β-galactosidase activity than wild-type cells at both the permissive and restrictive temperatures, indicating constitutive activation of the UPR pathway by the *rot1-2* mutation. Consistent with this, expression of *KAR2*, one of UPR target genes, was increased in *rot1-2* cells (Fig. 3B). Increased sensitivity to tunicamycin (Tm) was also observed. Tm is an inhibitor of *N*-glycosylation (*31*) and is known as a potent ER stressor. While wild-type cells grew slowly on YPD containing 0.5 μg/ml Tm, the *rot1-2* mutant did not grow at all (Fig. 3C).

In addition, *ROT1* expression was found to increase following treatment of wild-type cells with Tm or DTT (Fig. 3D, right panel). DTT induces ER stress by blocking disulfide bond formation. Treatment with Tm or DTT similarly increased *ROT1* expression in Δ*ire1* and Δ*hac1* strains (data not shown), indicating that upregulation of *ROT1* is mediated by a signalling pathway independent of *IRE1* and *HAC1* (*32*).

The rot1-2 Mutation Affects Various Aspects of Cellular Morphology—To further explore the physiological effects of the *rot1-2* mutation, the ultrastructure of the *rot1-2* mutant was analyzed by electron microscopy as described (*20*). Consistent with the findings of Machi *et al*. (*28*), an aberrant cell wall with a lower-than-normal electron density and an uneven thickness was observed (Fig. 4B). In addition, segregation of the septum was sometimes incomplete (data not shown). However, it should be noted that the abnormal intracellular structures observed in the *rot1-2* cells were not limited to the cell wall. When *rot1-2* cells were cultured at 37°C, the ER was occasionally found to have expanded in size (Fig. 4B). This phenotype has been associated with deformation of the nucleus (*33*).

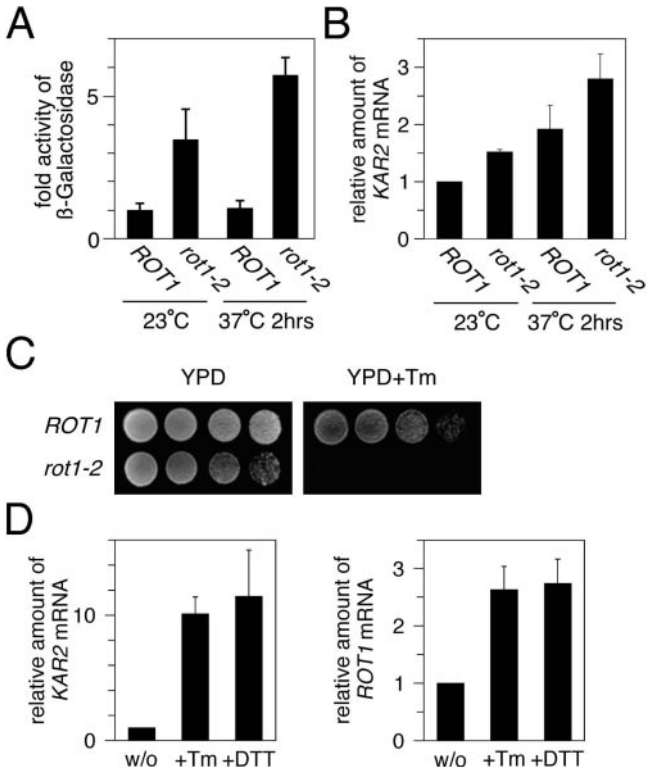

Fig. 3. ***ROT1* and ER stress.** (A) The UPR is activated in *rot1-2* mutants. The reporter plasmid pCZY1 (UPR element-*CYC1*p-*lacZ*) was transformed into wild-type (YM16) and *rot1-2* (YM18) cells. The resulting cells were cultured in liquid SC at 23°C and, when indicated, shifted to 37°C for 2 h. Cellular β-galactosidase activity was then measured. Mean values of ten experiments (normalized against that of the wild-type at 23°C) and SD are shown. (B) Expression of *KAR2* is increased in *rot1-2* mutants. Δ*rot1* cells carrying *ROT1* (YM19) or *rot1-2* (YM20) on a centromeric plasmid (pCL2-*ROT1* or pCL2-*rot1-2*) were grown in liquid YPD at 23°C and, when indicated, shifted to 37°C for 2 h. *KAR2* and *ACT1* mRNA were detected and measured by Northern blotting of total RNA. *KAR2* mRNA levels were normalized against that of *ACT1* mRNA, and the amount relative to that of YM19 incubated at 23°C is indicated. Averages and SD of three experiments are shown. (C) Growth of *rot1-2* mutant is abolished by Tm. YM16 and YM18 cells were spotted on YPD with or without Tm (0.5 μg/ml) in five-fold serial dilutions, and incubated at 30°C for 3 d. (D) Expression of *ROT1* is increased by ER stress. Wild-type cells (FY23) were grown in liquid YPD at 30°C, and treated with Tm (10 μg/ml) or DTT (10 mM) for 2 h. *KAR2*, *ROT1* and *ACT1* mRNAs were detected by Northern blotting of total RNA on the same membrane. *KAR2* and *ROT1* mRNA levels were normalized to that of *ACT1* mRNA, and the induction relative to non-treated cells is indicated. Averages and SD of four experiments are shown.

Moreover, extended and/or fragmented electron-dense, unidentified organelles were often observed (Fig. 4C and Fig. 4D).

When *rot1-2-HA* cells were incubated at 37°C and stained with anti-Kar2p antibody, punctate structures were observed along with the ER in 70–75% of the cells by fluorescence microscopy (compare cells in Fig. 4F with wild-type in Fig. 4E, which shows a typical staining pattern of the yeast ER as shown in Fig. 1F). Rot1-2p-HA was also distributed in the punctate structures, and their staining pattern was quite similar to that of BiP/Kar2p by double staining (compare Fig. 4H with Fig. 4F).

In addition, many small vesicles, which looked like autophagic bodies (*34*), were found to accumulate in the vacuole of *rot1-2* cells (Fig. 4L). Indeed, an autophagosome marker, GFP-Atg8p (*35*), was found to localize in dot-like structures in *rot1-2* cells (Fig. 4L), in a similar pattern to that observed in nutrient-starved wild-type cells treated with PMSF (Fig. 4M), an inhibitor of autophagic-body lysis. GFP-Atg8p was uniformly dispersed in the vacuole of wild-type cells (Fig. 4K), perhaps due to internalization of the autophagic bodies. By staining with quinacrine, which accumulates in acidic compartments, *rot1-2* cells were found to have a single, large and acidified vacuole (Fig. 4J) similar to that in wild-type cells (Fig. 4I). Therefore, the structure and acidification of the vacuole in *rot1-2* cells seem to be normal, while lysis of the autophagic bodies is likely defective. Taken together, *rot1-2* mutation affects not only cell wall synthesis, but also various aspects of cellular morphology and physiology.

The Combination of kar2-1 and rot1-2 Interferes with Folding and Glycosylation of Carboxypeptidase Y—CPY is a vacuolar soluble protease. The intracellular sorting of newly synthesized CPY is easily monitored by changes in mobility on SDS-PAGE (*36*). In the ER, four *N*-linked oligosaccharide chains are attached to CPY (ER form of proCPY; 67 kDa). If CPY is correctly folded in the ER, it is exported and undergoes elongation of the *N*-glycosyl chains in the Golgi (Golgi form of proCPY; 69 kDa) and cleavage of the N-terminal propeptide in the vacuole to generate mature CPY (61 kDa).

Folding of CPY in the ER was monitored by [^{35}S]-Met/Cys pulse-chase analysis. In all of the strains tested, the ER form was efficiently converted to the Golgi form and then into the mature form within 20 min (Fig. 5, A and B), but this conversion was slightly slower in the *kar2-1* single mutant and in the *kar2-1 rot1-2* double mutant. In the *kar2-1 rot1-2* double mutant, a portion of CPY was not glycosylated (Fig. 5B, arrowheads).

We next asked if post-translocational folding of reduced CPY is impaired in these mutants. Because CPY requires intramolecular disulfide bond formation for proper folding in the ER, newly-synthesized CPY remains unfolded in the ER when cells are treated with DTT. Upon removal of DTT, reduced CPY begins to fold in a Kar2p-dependent process (*8*). Cells were treated with DTT prior to pulse-labelling, after which the DTT was removed at the beginning of the chase period. In wild-type cells, CPY was gradually converted to the mature form. Similar results were obtained for the *kar2-1* and *rot1-2* single mutants (Fig. 5, C and D). However, in the case of the *kar2-1 rot1-2* double mutant, the result was strikingly different. First, even at time 0, multiple protein bands were observed. Because the EndoH digestion gave a single band with the same mobility as proCPY (dg-E in Fig. 5E), we presume that a portion of the reduced CPY was under-glycosylated (nascent protein translocation was normal; data not shown). Second, the SDS-PAGE banding pattern did not change during the chase period, which indicates that reduced CPY does not undergo additional modification but remains unfolded in the ER. Thus, we suggest that reduced CPY is severely denatured so

that it loses folding competency and is *N*-glycosylated inefficiently.

Rot1p Forms a Complex with Kar2p In Vivo—To investigate a possible interaction between Kar2p and Rot1p, co-immunoprecipitation of Kar2p with Rot1p was tested *in vivo*. Cells expressing Rot1p-HA were lysed and subjected to non-denaturing immunoprecipitation with anti-Kar2p antibody, and co-precipitated Rot1p-HA was detected by anti-HA Western blotting. As shown in Fig. 6, association of Kar2p and Rot1p-HA was observed (compare lanes 2 and 1) and was found to increase dramatically by treatment of cells with DTT or Tm (lanes 3–6). The drug treatments increased the total cellular amount of Kar2p and Rot1p-HA by approximately 1.4 fold only, respectively. The rot1-2p-HA mutant protein was also found to co-precipitate with Kar2p in a similar manner (data not shown).

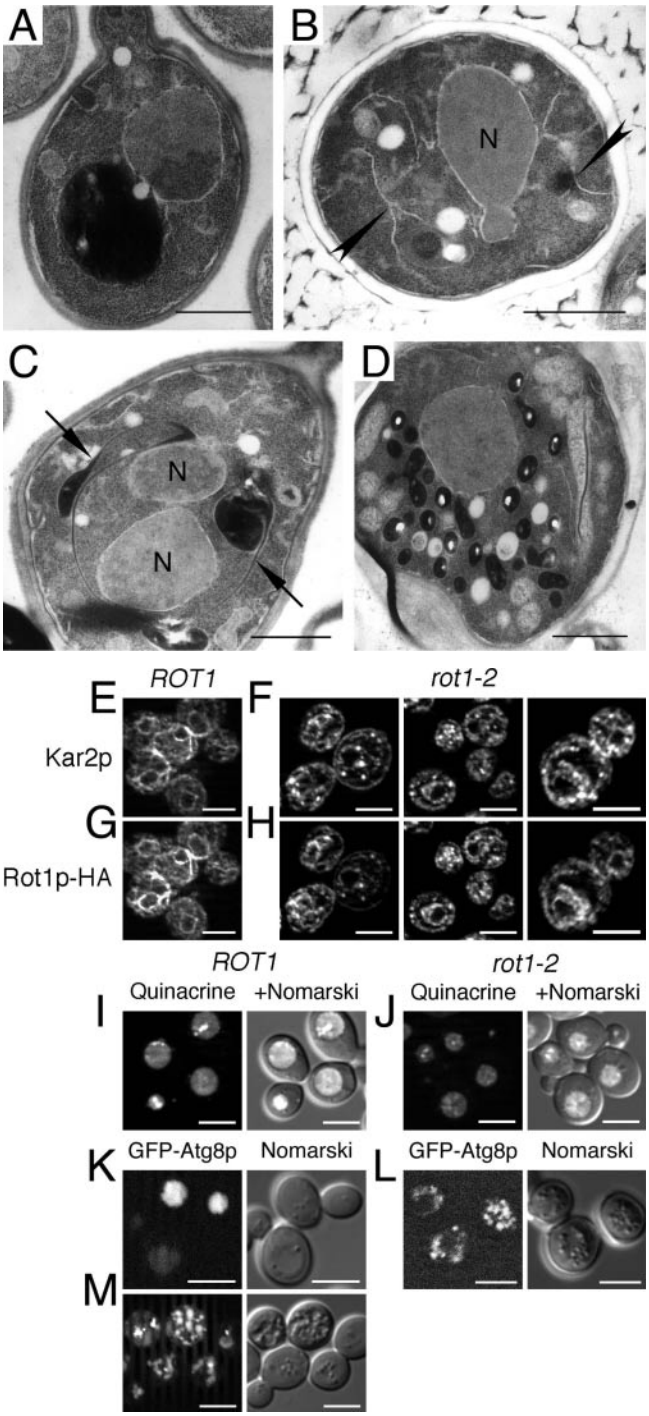

DISCUSSION

In this report, we have described basic characterization of Rot1p and analysis of the *rot1-2* mutant. Rot1p is suggested to participate in protein folding (maturation) in the ER together with Kar2p. As shown in Fig. 1, A and D—F, the majority of Rot1p is an ER-localized transmembrane protein. Rot1p possesses one transmembrane domain at the C terminus, and multiple *N*-glycosyl chains of Rot1p (Fig. 1C) indicate that this protein faces the lumen. These characteristics of Rot1p are consistent with our conclusion that Rot1p possibly acts together with BiP/Kar2p. A minor portion of Rot1p, sRot1p, appears to be a glycosylation variant of Rot1p having two oligosaccharides (Fig. 1C), and its cellular distribution seems to be different from that of Rot1p (Fig. 1E). So far, the function and importance of sRot1p are not clear.

Phenotypic analysis of a *ROT1* mutant allele (*rot1-2*) suggests involvement of Rot1p in protein folding. First, *ROT1* exhibited significant genetic interactions with several ER chaperone genes, including *KAR2*, *CNE1*, *SCJ1* and *LHS1* (Fig. 2). Second, the *rot1-2* mutation caused constitutive activation of the UPR pathway (Fig. 3A, B), which implies accumulation of unfolded proteins in the ER. Third, expansion of the ER and deformation of the nucleus were occasionally observed by electron microscopic analysis of *rot1-2* cells (Fig. 4B), which suggest impairment of ER function (*33*). Fourth, localization of Kar2p in punctate structures (Fig. 4F) also suggests impairment of protein folding in the ER of the *rot1-2* mutant, because a similar distribution of Kar2p was observed when unfolded proteins aggregated in the ER (*37*). Finally, a model client protein, reduced CPY, failed to fold in the *kar2-1 rot1-2* double mutant (Fig. 5D). This also supports our hypothesis that

Fig. 4. **The *rot1-2* mutation affects various aspects of cellular morphology.** (A–D) Wild-type (YM16; A) and *rot1-2* mutants (YM18; B–D) were grown in liquid YPD at 23°C, and shifted to 37°C for 2 (B, C) or 6 h (A, D). Cells were then analyzed by electron microscopy. Arrows, extended electron-dense organelles; N, deformed nucleus; bars, 1 μm. (E–H) Kar2p and rot1-2p are co-localized to punctate structures. Δ*rot1* cells expressing Rot1p-HA (YM13) or rot1-2p-HA (YM14) were incubated as in A–D (shifted to 37°C for 6 h). Cells were fixed and subjected to indirect double immunofluorescence staining with rabbit anti-Kar2p and mouse anti-HA antibodies. (I, J) The *rot1-2* mutant has a single acidified vacuole at 37°C, similar to the wild- type. YM16 and YM18 cells were treated as in A–D (shifted to 37°C for 5.5 h). Na-PO_4 (pH 7.4) and quinacrine were then added to a final concentration of 50 mM each, and cells were further incubated for 30 min and observed by fluorescence microscopy using an FITC filter. Nomarski images are merged in the right panel. (K–M) Autophagic bodies accumulate in *rot1-2* cells. YM16 (K) or YM18 (L) cells carrying pL-*GFP-ATG8* were incubated in liquid SC at 37°C for 6 h, and GFP fluorescence was observed. Nomarski images are also shown in the right panel. In M, YM16 cells carrying pL-*GFP-ATG8* were incubated in liquid SD lacking ammonium sulfate but containing 1 mM PMSF at 30°C for 6 h, and observed similarly. Bars in E–M, 5 μm.

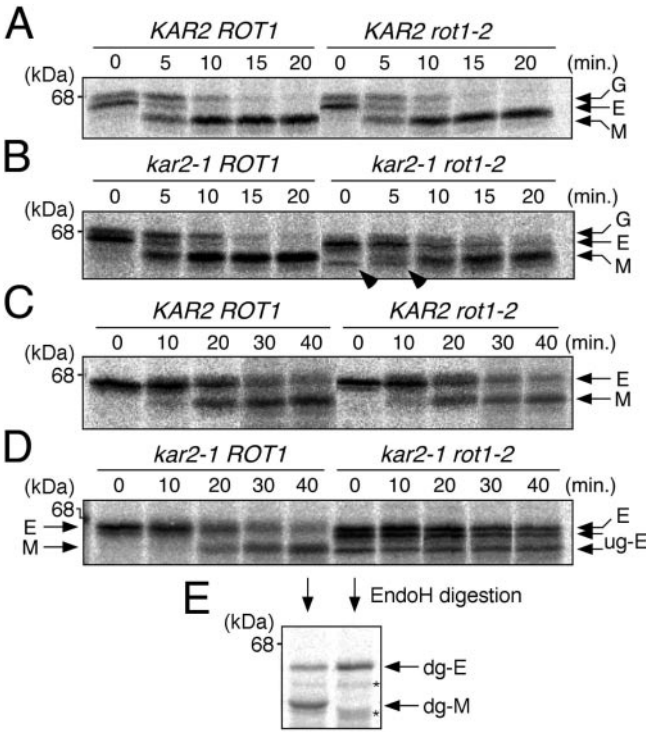

Fig. 5. **Defect in protein folding in the *kar2-1 rot1-1* double mutant.** (A, B) Yeast strains (derived from YM11; see Fig. 2A) were grown in liquid SC without Met and Cys at 23°C. Cells were then incubated at 37°C for 30 min, labelled with [^{35}S]-Met/Cys for 5 min and chased for the period indicated above each panel. Immunoprecipitated CPY was analyzed by SDS-PAGE (8%) and autoradiography. (C, D) The combination of *kar2-1* and *rot1-2* causes impaired maturation of reduced CPY. Prior to pulse-labelling, cells were incubated at 37°C for 15 min. DTT was then added to a final concentration of 5 mM to the cultures, which were further incubated for 15 min. The cells were labeled for 10 min, and DTT was washed out at the beginning of the chase period. (E) Immunoprecipitated CPY (reduced CPY of *kar2-1 ROT1* cells chased for 40 min. and that of *kar2-1 rot1-2* cells without chase) was treated with EndoH and analysed. E, ER form; G, Golgi form; M, mature CPY; arrowheads in B, unglycosylated proCPY; ug-E, underglycosylated ER form; dg-E, deglycosylated ER form; dg-M, deglycosylated mature CPY; asterisks in E, non-specific signals.

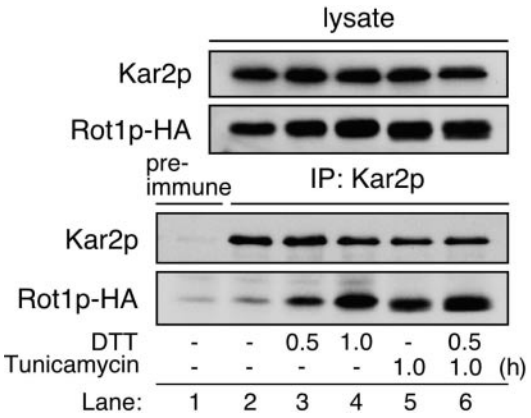

Fig. 6. **Interaction of Kar2p and Rot1p.** Δ*rot1* cells expressing Rot1p-HA (YM13) were grown at 30°C, and Kar2p was immunoprecipitated under non-denaturing conditions. After treatment with EndoH, the immunocomplex was subjected to anti-Kar2p and anti-HA western blotting. Where indicated, cells were incubated with DTT (10 mM) and/or Tm (10 μg/ml) before lysis.

Rot1p functions together with Kar2p, and we obtained further evidence for it.

The allele specificity of *kar2* mutants that exhibit a synthetic growth defect with *rot1-2* (Fig. 2A) implies that Kar2p and Rot1p interact directly to cooperate in a biological process(es). We also demonstrated that Kar2p and Rot1p formed a complex *in vivo*, which was dramatically enhanced by treatment of cells with DTT or Tm (Fig. 6). This suggests ternary complex formation among Kar2p, Rot1p and a client protein. Alternatively, Rot1p may be recognized by Kar2p as an unfolded protein; however, Rot1p is unlikely to be damaged by DTT, because the two cysteine residues in Rot1p (Cys 90 and 127) were found not to be required for the function (and probably structure) of this protein (*ROT1*[C90S/C127S] rescued Δ*rot1*; data not shown).

ROT1 was initially reported as a factor important for 1,6-β-glucan synthesis (*27*, *28*). We also found that the cell wall structure of *rot1-2* cells was severely distorted (Fig. 4B). However, based on the other findings described in this report, we believe that these abnormalities in the cell wall are secondary effects of loss of Rot1p functions, as protein(s) important for cell wall synthesis may be poorly folded or matured in *rot1-2* cells. The impairment of lysis of autophagic bodies in the *rot1-2* cells (Fig. 4L) can be interpreted similarly. Identification of Rot1p-dependent proteins and analysis of their folding are required to assess our hypothesis, and may clarify not only the detailed functions of Rot1p but also new aspects of BiP/Kar2p-mediated protein folding in the ER.

We thank Drs. Ed C. Hurt (Universitat Heidelberg), Mark D. Rose (Princeton University), and Fred Winston (Harvard Medical School) for yeast strains, Dr. Randy Schekman (University of California, Berkeley) for anti-Sec61p antibody, Miki Matsumura and Hisayo Masuda for technical assistance, and Dr. Ian Smith for critical reading of this manuscript. This work was supported by Grants-in-Aids for Scientific Research on Priority Areas (14037240 to K. K., 15030232 to Y. K.) and for 21st Century COE Research from MEXT, and JSPS.KAKENHI (15570160 to Y. K.). M.T. was supported by a postdoctoral fellowship from KAKENHI (14037240).

REFERENCES

1. Bukau, B. and Horwich, A.L. (1998) The Hsp70 and Hsp60 chaperone machines. *Cell* **92**, 351–366
2. Kelley, W.L. (1998) The J-domain family and the recruitment of chaperone power. *Trends Biochem. Sci.* **23**, 222–227
3. Shomura, Y., Dragovic, Z., Chang, H.C., Tzvetkov, N., Young, J.C., Brodsky, J.L., Guerriero, V., Hartl, F.U., and Bracher, A. (2005) Regulation of Hsp70 function by HspBP1: structural analysis reveals an alternate mechanism for Hsp70 nucleotide exchange. *Mol. Cell* **17**, 367–379
4. Ballinger, C.A., Connell, P., Wu, Y., Hu, Z., Thompson, L.J., Yin, L.Y., and Patterson, C. (1999) Identification of CHIP, a

novel tetratricopeptide repeat-containing protein that interacts with heat shock proteins and negatively regulates chaperone functions. *Mol. Cell. Bio.l* **19**, 4535–4545
5. Hohfeld, J., Minami, Y., and Hartl, F.U. (1995) Hip, a novel cochaperone involved in the eukaryotic Hsc70/Hsp40 reaction cycle. *Cell* **83**, 589–598
6. Frydman, J. and Hohfeld, J. (1997) Chaperones get in touch: the Hip-Hop connection. *Trends Biochem. Sci.* **22**, 87–92
7. Corsi, A.K. and Schekman, R. (1997) The lumenal domain of Sec63p stimulates the ATPase activity of BiP and mediates BiP recruitment to the translocon in Saccharomyces cerevisiae. *J. Cell Biol.* **137**, 1483–1493
8. Simons, J.F., Ferro-Novick, S., Rose, M.D., and Helenius, A. (1995) BiP/Kar2p serves as a molecular chaperone during carboxypeptidase Y folding in yeast. *J. Cell Biol.* **130**, 41–49
9. Fewell, S.W., Travers, K.J., Weissman, J.S. and Brodsky, J.L. (2001) The action of molecular chaperones in the early secretory pathway. *Annu. Rev. Genet.* **35**, 149–91
10. Ellgaard, L., Molinari, M., and Helenius, A. (1999) Setting the standards: quality control in the secretory pathway. *Science* **286**, 1882–8
11. Nishikawa, S.I., Fewell, S.W., Kato, Y., Brodsky, J.L., and Endo, T. (2001) Molecular chaperones in the yeast endoplasmic reticulum maintain the solubility of proteins for retrotranslocation and degradation. *J. Cell Biol.* **153**, 1061–1070
12. Silberstein, S., Schlenstedt, G., Silver, P.A., and Gilmore, R. (1998) A role for the DnaJ homologue Scj1p in protein folding in the yeast endoplasmic reticulum. *J. Cell Biol.* **143**, 921–933
13. Kabani, M., Beckerich, J.M., and Gaillardin, C. (2000) Sls1p stimulates Sec63p-mediated activation of Kar2p in a conformation-dependent manner in the yeast endoplasmic reticulum. *Mol. Cell. Biol.* **20**, 6923–6934
14. Steel, G.J., Fullerton, D.M., Tyson, J.R., and Stirling, C.J. (2004) Coordinated activation of Hsp70 chaperones. *Science* **303**, 98–101
15. Tyson, J.R. and Stirling, C.J. (2000) *LHS1* and *SIL1* provide a lumenal function that is essential for protein translocation into the endoplasmic reticulum. *EMBO J.* **19**, 6440–6452
16. Craven, R.A., Tyson, J.R., and Stirling, C.J. (1997) A novel subfamily of Hsp70s in the endoplasmic reticulum. *Trends Cell Biol.* **7**, 277–282
17. Saris, N., Holkeri, H., Craven, R.A., Stirling, C.J., and Makarow, M. (1997) The Hsp70 homologue Lhs1p is involved in a novel function of the yeast endoplasmic reticulum, refolding and stabilization of heat-denatured protein aggregates. *J. Cell Biol.* **137**, 813–824
18. Kaiser, C., Michaelis, S., and Mitchell, A. (1994) *Methods in Yeast Genetics*, Cold Spring Harbor Laboratory Press, Cold Spring Harbor, NY
19. Wimmer, C., Doye, V., Grandi, P., Nehrbass, U., and Hurt, E.C. (1992) A new subclass of nucleoporins that functionally interact with nuclear pore protein NSP1. *EMBO J.* **11**, 5051–5061
20. Higashio, H., Kimata, Y., Kiriyama, T., Hirata, A., and Kohno, K. (2000) Sfb2p, a yeast protein related to Sec24p, can function as a constituent of COPII coats required for vesicle budding from the endoplasmic reticulum. *J. Biol. Chem.* **275**, 17900–17908
21. Kimata, Y., Kimata, Y.I., Shimizu, Y., Abe, H., Farcasanu, I.C., Takeuchi, M., Rose, M.D., and Kohno, K. (2003) Genetic evidence for a role of BiP/Kar2 that regulates Ire1 in response to accumulation of unfolded proteins. *Mol. Biol. Cell* **14**, 2559–2569
22. Craven, R.A., Egerton, M., and Stirling, C.J. (1996) A novel Hsp70 of the yeast ER lumen is required for the efficient translocation of a number of protein precursors. *EMBO J* **15**, 2640–2650
23. Roberg, K.J., Rowley, N., and Kaiser, C.A. (1997) Physiological regulation of membrane protein sorting late in the secretory pathway of *Saccharomyces cerevisiae*. *J. Cell Biol.* **137**, 1469–1482
24. Kohno, K., Normington, K., Sambrook, J., Gething, M.J., and Mori, K. (1993) The promoter region of the yeast *KAR2* (BiP) gene contains a regulatory domain that responds to the presence of unfolded proteins in the endoplasmic reticulum. *Mol. Cell. Biol.* **13**, 877–890
25. Kimata, Y., Oikawa, D., Shimizu, Y., Ishiwata-Kimata, Y., and Kohno, K. (2004) A role for BiP as an adjustor for the endoplasmic reticulum stress-sensing protein Ire1. *J. Cell Biol.* **167**, 445–456
26. Brodsky, J.L., Werner, E.D., Dubas, M.E., Goeckeler, J.L., Kruse, K.B., and McCracken, A.A. (1999) The requirement for molecular chaperones during endoplasmic reticulum-associated protein degradation demonstrates that protein export and import are mechanistically distinct. *J. Biol. Chem* .**274**, 3453–3460
27. Bickle, M., Delley, P.A., Schmidt, A., and Hall, M.N. (1998) Cell wall integrity modulates RHO1 activity via the exchange factor ROM2. *EMBO J.* **17**, 2235–2245
28. Machi, K., Azuma, M., Igarashi, K., Matsumoto, T., Fukuda, H., Kondo, A., and Ooshima, H. (2004) Rot1p of *Saccharomyces cerevisiae* is a putative membrane protein required for normal levels of the cell wall 1,6-beta-glucan. *Microbiology* **150**, 3163–3173
29. Scidmore, M.A., Okamura, H.H., and Rose, M.D. (1993) Genetic interactions between *KAR2* and *SEC63*, encoding eukaryotic homologues of DnaK and DnaJ in the endoplasmic reticulum. *Mol. Biol. Cell* **4**, 1145–1159
30. Parlati, F., Dominguez, M., Bergeron, J.J., and Thomas, D.Y. (1995) *Saccharomyces cerevisiae CNE1* encodes an endoplasmic reticulum (ER) membrane protein with sequence similarity to calnexin and calreticulin and functions as a constituent of the ER quality control apparatus. *J. Biol. Chem.* **270**, 244–253
31. Takatsuki, A., Kohno, K., and Tamura, G. (1975) Inhibition of biosynthesis of polyisoprenol sugars in chick embryo microsomes by tunicamycin. *Agric. Biol. Chem.* **39**, 2089–2091
32. Schroder, M., Clark, R., and Kaufman, R.J. (2003) IRE1- and HAC1-independent transcriptional regulation in the unfolded protein response of yeast. *Mol. Microbiol.* **49**, 591–606
33. Kimata, Y., Lim, C.R., Kiriyama, T., Nara, A., Hirata, A., and Kohno, K. (1999) Mutation of the yeast epsilon-COP gene *ANU2* causes abnormal nuclear morphology and defects in intracellular vesicular transport. *Cell Struct. Funct.* **24**, 197–208
34. Takeshige, K., Baba, M., Tsuboi, S., Noda, T., and Ohsumi, Y. (1992) Autophagy in yeast demonstrated with proteinase-deficient mutants and conditions for its induction. *J. Cell Biol.* **119**, 301–311
35. Kirisako, T., Baba, M., Ishihara, N., Miyazawa, K., Ohsumi, M., Yoshimori, T., Noda, T., and Ohsumi, Y. (1999) Formation process of autophagosome is traced with Apg8/Aut7p in yeast. *J. Cell Biol.* **147**, 435–446
36. Stevens, T., Esmon, B., and Schekman, R. (1982) Early stages in the yeast secretory pathway are required for transport of carboxypeptidase Y to the vacuole. *Cell* **30**, 439–448
37. Nakatsukasa, K., Okada, S., Umebayashi, K., Fukuda, R., Nishikawa, S., and Endo, T. (2004) Roles of O-mannosylation of aberrant proteins in reduction of the load for endoplasmic reticulum chaperones in yeast. *J. Biol. Chem.* **279**, 49762–49772